

SUPPLEMENTAL MATERIAL

Mycobacterium tuberculosis* NmtR harbors a nickel sensing site with parallels to *Escherichia coli* RcnR

Hermes Reyes-Caballero, Chul Won Lee and David P. Giedroc

Supplementary Tables S1-S3; Supplementary Figures S1-S7

Supplementary References

Table S1. Putative and known metal ion transporters in *Mtb* with known transcriptional regulators

Family	Transporter	Regulator	Inducer	Family	Ref
<i>P-ATPase (metal efflux)</i>	<i>ctpG</i> (rv1992c)	CmtR	Pb(II)/Cd(II)	ArsR/SmtB	¹
	<i>ctpJ</i> (rv3743c)	NmtR	Ni(II)/Co(II)	ArsR/SmtB	²
	<i>ctpV</i> (rv0969)	CsoR	Cu(I)	CsoR/RcnR	³
<i>Cation diffusion facilitator (metal efflux)</i>	<i>cdf</i> (rv2025c)	KmtR	Ni(II)/Co(II)	ArsR/SmtB	⁴
<i>ABC transporters</i>					
<i>metal uptake</i>	<i>irtAB</i> (rv1348-1349)	IdeR	Fe(II)	DtxR/IdeR	⁵
<i>metal uptake</i>	<i>znuAB</i> (rv2059, rv2060, rv2061c)	FurB (Zur)	Zn(II)	Fur	⁶

Table S2. Electrospray ionization-mass spectrometry (LC-ESI-MS) of apo wild-type and variants NmtR.^a

NmtR variant	Expected MW (Da) ^b	MW observed (Da)	Δ (amu) ^c
WT	12835.6	12703.1	132.5
H3Q	12826.5	12694.7	131.8
D91Q	12848.6	12717.4	131.2
H93Q	12826.5	12695.7	130.8
H107Q	12826.5	12695.7	130.8
H109Q	12826.5	12695.7	130.8
D114Q	12848.6	12717.8	130.8
H116Q	12826.5	12695.6	130.0
Δ111NmtR	11914.6	11784.6	130.0

^aConditions: Protein concentration 30-80 μM, C4 column filtered. ^bMolecular weight expected for residues 1-120. ^cFully consistent with Met1 processed.

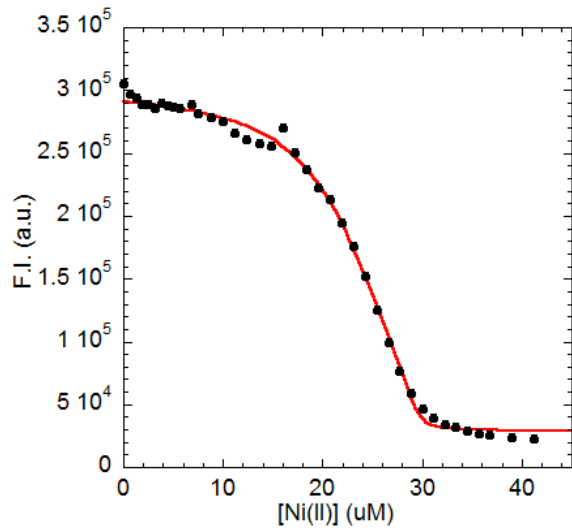
Table S3. Metal induced DNA binding by H104Q NmtR

NmtR H104Q	$\Delta r_{\text{max}}^{\text{a}}$	$\Delta r_{\text{obs}}^{\text{b}}$	$K_{\text{DNA}}^{\text{c}}$ ($\times 10^9 \text{ M}^{-1}$)	$\Delta G_c^{\text{c,d}}$ (kcal mol $^{-1}$)
<i>apo</i> ^e		0.004	0.14 (± 0.01)	-
<i>10 μM metal</i>				
Ni(II)		0.007	0.37 (± 0.04)	-0.6 (± 0.1)
Co(II)		0.008	0.42 (± 0.04)	-0.6 (± 0.01)
Zn(II)		0.007	0.33 (± 0.01)	-0.5 (± 0.04)
<i>100 μM metal</i>				
Ni(II)	0.011	0.010	1.0 (± 0.1)	-1.2 (± 0.1)
Co(II)		0.007	0.23 (± 0.01)	-0.29 (± 0.04)
Zn(II)		0.010	0.13 (± 0.01)	0
<i>Nonspecific DNA, f 100 μM metal</i>				
Ni(II)		0.001	0.01(± 0.002)	-

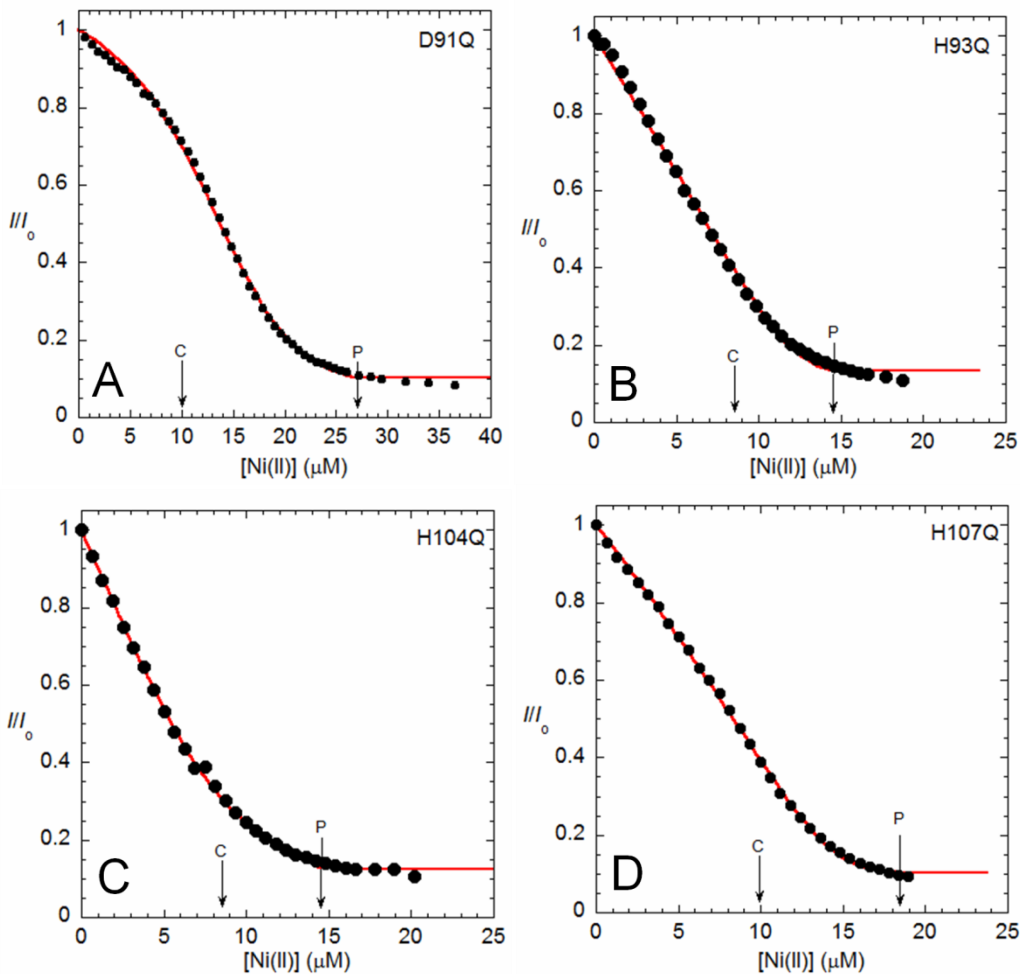
Conditions: 10mM Hepes, pH 7, 0.4 M NaCl, 25.0 °C. Excess salmon sperm DNA.

^a Δr_{max} = anisotropy fix as maximal response in the fit and normalization^b Δr_{obs} = anisotropy change at maximum measured protein concentration^c $\Delta G_c = -RT \ln(K_{\text{DNA-Ni}}/K_{\text{DNA-apo}})$ ^dFor comparison ΔG_c Ni(II)NmtR wild-type = 2.7 (± 0.2) kcal mol $^{-1}$ ^eFor determination of *apo* K_{DNA} 500 μM EDTA was added to the binding reaction.^fSequence in the oligo is not related to NmtR

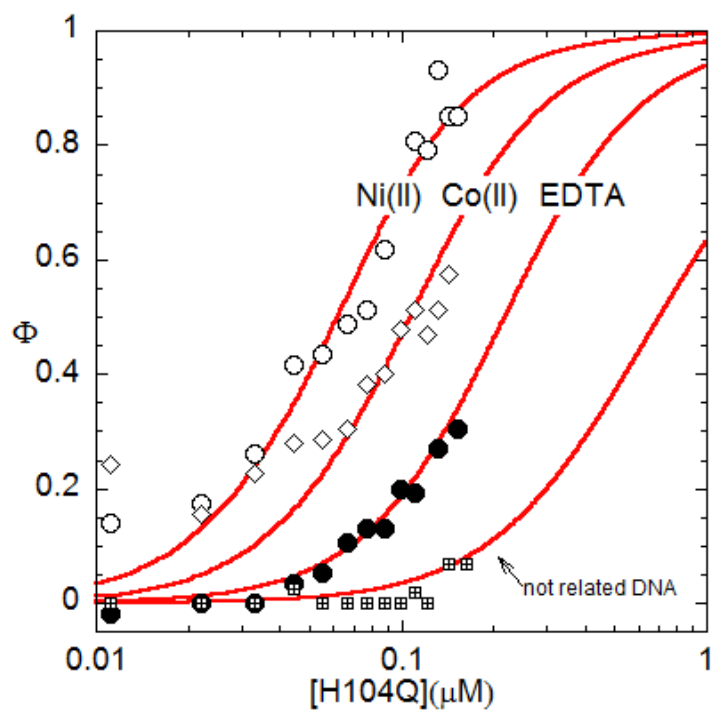
Supplementary Figure S1. Determination of the mag-fura-2 (mf2) binding affinity for Ni(II). Binding affinity of mf2 for Ni(II) was obtained from a competition experiment with NTA. The binding isotherm of Ni(II) titration into mf2 depicted as the total fluorescence intensity (F.I.). The red line represents a non-linear least-square fit to a 1:1 Ni(II):mf2 binding model. The calculated value $K_{Mf2-Ni} = 2.0 (\pm 0.1) \times 10^7 M^{-1}$. Conditions: [NTA] = 20 μM and [mf2] = 9.7 μM , pH 7.0, 0.4 M NaCl, 25.0 °C.



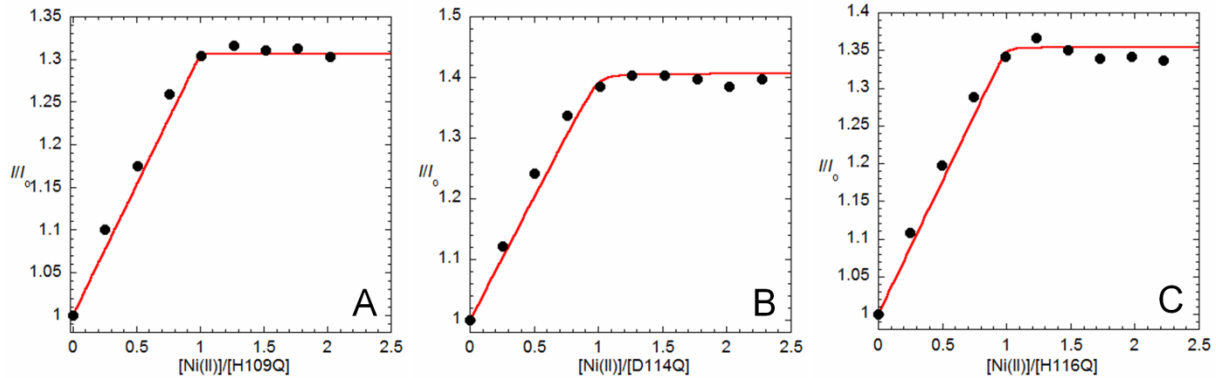
Supplementary Figure S2. Ni(II) binding to NmtR variants harboring single α 5-site Gln substitutions. Ni(II) Binding is monitored by measuring the quenching of the mf2 fluorescence. Red lines represent non-linear least square fit to a 2:1(Ni(II):dimer) binding model. All the K_{Ni} values are given in Table 2.2. An arrow labeled C represents the concentration of Ni(II) sites for the chelator alone and an arrow labeled P points at the total concentration of Ni sites assuming a 1:1 Ni:NmtR protomer binding stoichiometry (both in μ M). [Concentrations] (μ M); (A) [D91Q] = 17 [mf2] = 10, (B) [H93Q] = 6.0, [mf2] = 8.5, (C) [H104Q] = 6.0, [mf2] = 8.5, (D) [H107Q] = 7.5, [mf2] = 10.



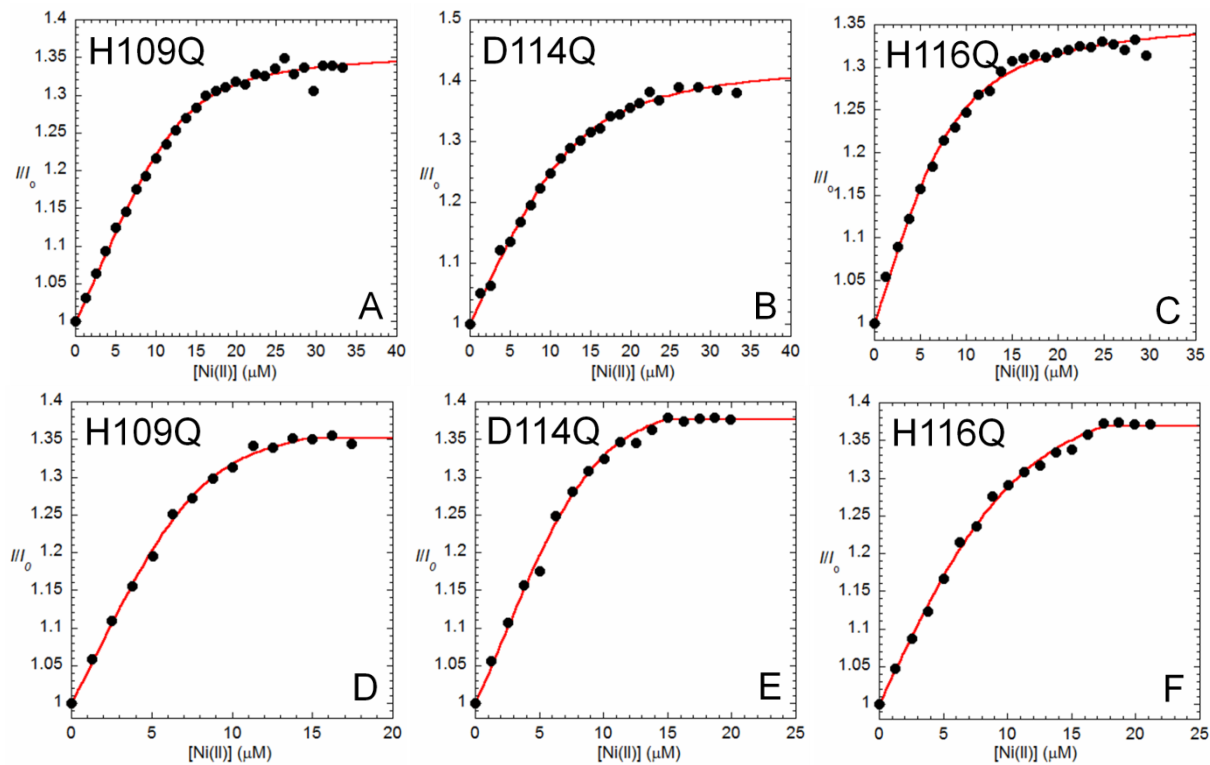
Supplementary Figure S4. Distinct allosteric regulation of H104Q Ni(II)NmtR. Depict are binding isotherms of fluorescence anisotropy experiments used to monitor DNA binding. Open and closed symbols represent metal or apo- form, respectively. The red line represents non-linear least-square fits to a model where a dissociable dimer binds to a single DNA probe. The total anisotropy change is normalized to the Ni(II) NmtR value (Δr_{\max}) so for each instance the anisotropy change observed (Δr_{obs}) is a fraction of that for Ni(II)-NmtR. Table 2.6 gives the K_{DNA} values calculated from this analysis, along with Δr_{\max} . Key to notation (as indicated in the figure): Ni(II); open circles, Co(II); diamonds, Non related DNA, crossed squares. The experiments were performed in excess of nonspecific DNA competitor and the data shown were obtained in the presence of excess (100 μM) metal.



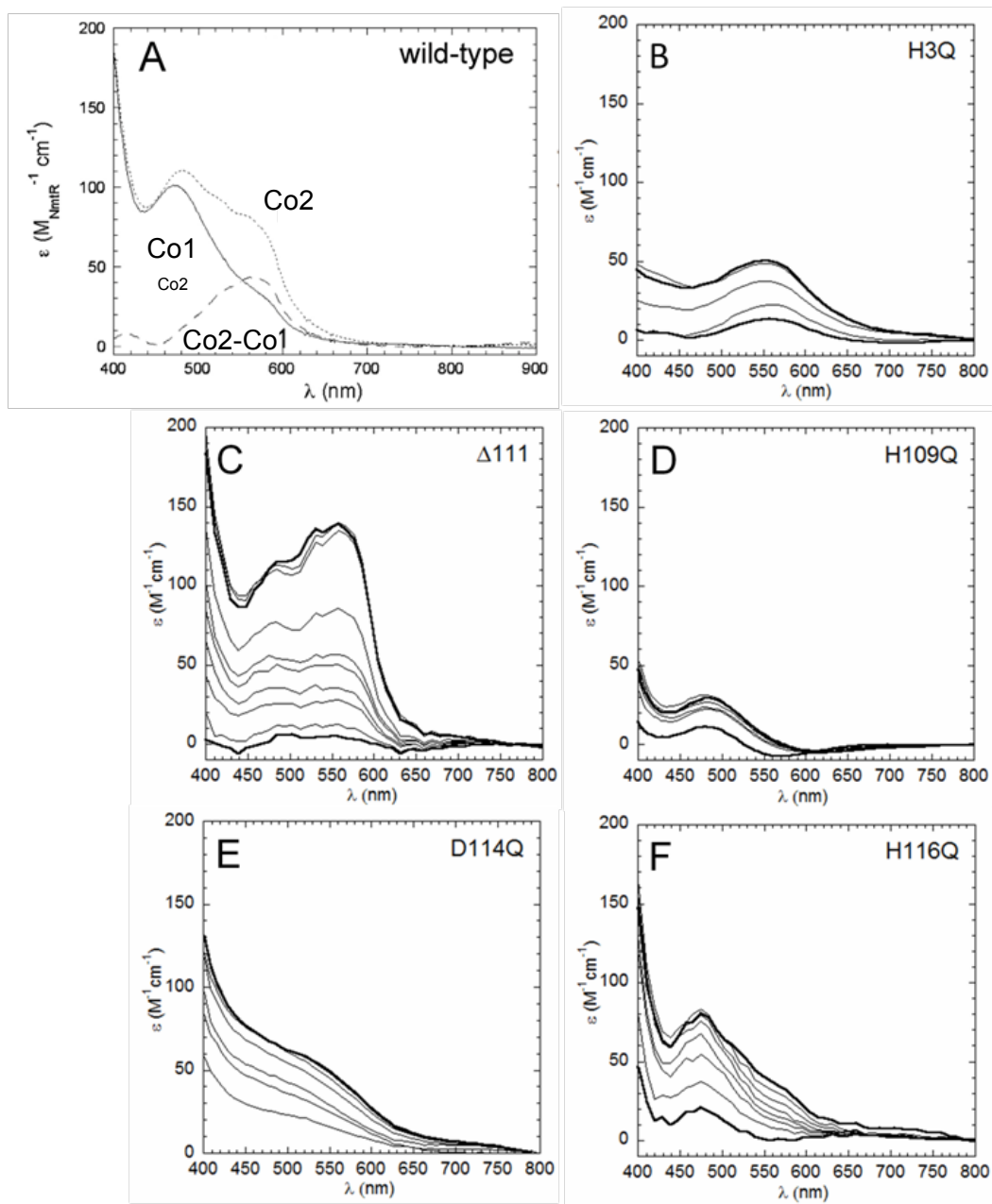
Supplementary Figure S5. Binding of Ni(II) to C-terminal NmtR variants. Ni(II) binding isotherm as monitored by the intrinsic fluorescence intensity change (I/I_0). The red line represents non-linear least-square fits to a 1:1 (Ni(II):monomer) binding model. (A) H109Q ($K_{Ni} \sim 1.65 \times 10^8 M^{-1}$), (B) D114Q ($K_{Ni} \sim 6.4 \times 10^8 M^{-1}$), (C) H116Q ($K_{Ni} \sim 3.30 \times 10^8 M^{-1}$). [Concentrations] (μM): (A) –(C) 5.0 μM .



Supplementary Figure S6. NTA and EGTA Ni(II) competition experiments with C-terminal missense mutant NmtRs. Ni(II) binding was monitored by the intensity of the intrinsic fluorescence change (I/I_0), in the presence of NTA (A)-(C) or EGTA (D)-(F). The red line represents non-linear least-square fits to a 2:1 (Ni(II):dimer) binding model. The results of the fits are given in the text (Table 2, main text). (A) 10 μM H109Q NmtR and 20 μM NTA, (B) 10 μM D114Q NmtR and 20 μM NTA, (C) 5.0 μM H116Q NmtR and 12.5 μM NTA, (D) 5.0 μM H109Q NmtR and 10 μM EGTA, (E) 5.0 μM D114Q NmtR and 10 μM EGTA, (F) 5.0 μM H116Q NmtR and 12.5 μM EGTA. Apparent stepwise Ni(II) binding affinities $K_{\text{Ni}1}$, $K_{\text{Ni}2}$ ($\times 10^{10} \text{ M}^{-1}$); (A) 0.50 (± 0.10), 1.00 (± 0.01), (B) 0.80 (± 0.10), 0.45 (± 0.04), (C) 0.60 (± 0.10), 0.60 (± 0.05), (D) 1.00 (± 0.04), 1.00 (± 0.04), (E) 0.72 (± 0.04), 0.72 (± 0.04), (F) 0.95 (± 0.01), 0.50 (± 0.07).



Supplementary Figure S7. Co(II) electronic absorption spectra of H3Q and C-terminal variant NmtRs. Concentrations of each NmtR is given in μM monomer. (A) Previously published spectra for wild-type Co₁-NmtR dimer (Co1), Co₂-NmtR dimer (Co2), subtracted Co₂-Co₁ wild-type NmtR (Co2-Co1).² (B) [H3Q NmtR] 50; (C) [Δ 111 NmtR] 140; (D) [H109Q NmtR] 50; (E) [D114Q NmtR] 50; (F) [H116Q NmtR] 50.



REFERENCES

- (1) ^aCavet, J. S., Graham, A. I., Meng, W. M. & Robinson, N. J. (2003). A cadmium-lead-sensing ArsR-SmtB repressor with novel sensory sites - Complementary metal discrimination by

- NmtR and CmtR in a common cytosol. *J. Biol. Chem.* 278, 44560-44566; ^bWang, Y., Hemmingsen, L. & Giedroc, D. P. (2005). Structural and functional characterization of *Mycobacterium tuberculosis* CmtR, a Pb^{II}/Cd^{II}-sensing SmtB/ArsR metalloregulatory repressor. *Biochemistry* 44, 8976-88.
- (2) Cavet, J. S., Meng, W., Pennella, M. A., Appelhoff, R. J., Giedroc, D. P. & Robinson, N. J. (2002). A nickel-cobalt-sensing ArsR-SmtB family repressor. Contributions of cytosol and effector binding sites to metal selectivity. *J. Biol. Chem.* 277, 38441-8.
- (3) Liu, T., Ramesh, A., Ma, Z., Ward, S. K., Zhang, L. M., George, G. N., Talaat, A. M., Sacchettini, J. C. & Giedroc, D. P. (2007). CsoR is a novel *Mycobacterium tuberculosis* copper-sensing transcriptional regulator. *Nat. Chem. Biol.* 3, 60-68.
- (4) Campbell, D. R., Chapman, K. E., Waldron, K. J., Tottey, S., Kendall, S., Cavallaro, G., Andreini, C., Hinds, J., Stoker, N. G., Robinson, N. J. & Cavet, J. S. (2007). Mycobacterial Cells Have Dual Nickel-Cobalt Sensors. *J. Biol. Chem.* 282, 32298-32310.
- (5) Rodriguez, G. M. & Smith, I. (2006). Identification of an ABC transporter required for iron acquisition and virulence in *Mycobacterium tuberculosis*. *J. Bacteriol.* 188, 424-30.
- (6) ^aCanneva, F., Branzoni, M., Riccardi, G., Provvedi, R. & Milano, A. (2005). Rv2358 and FurB: Two Transcriptional Regulators from *Mycobacterium tuberculosis* which respond to Zinc. *J. Bacteriol.* 187, 5837-5840; ^bLucarelli, D., Russo, S., Garman, E., Milano, A., Meyer-Klaucke, W. & Pohl, E. (2007). Crystal Structure and Function of the Zinc Uptake Regulator FurB from *Mycobacterium tuberculosis*. *J. Biol. Chem.* 282, 9914-9922.